High Temp. Mater. Proc., Vol. **30** (2011), pp. 425–434 DOI 10.1515/HTMP.2011.064

Novel Recycling Process of Mn by Sulfurization of Molten Slag from a By-Product of Steelmaking Process

Sun-Joong Kim,[1] **Hiroyuki Shibata,**[2,*] **Nobuhiro Maruoka,**[2] **Shinya Kitamura**[2] **and Katsunori Yamaguchi**[3]

[1] Graduate School of Engineering, Tohoku University, Sendai, Japan

[2] Institute of Multidisciplinary Research for Advanced Materials, Tohoku University, Sendai, Japan

[3] Iwate University, Morioka, Japan

Abstract. We propose a novel process to recycle Mn from steelmaking slag. The first step is to sulfurize the slag, producing a liquid sulfide phase (matte) without P. High-purity Fe-Mn alloys can then be made by desulfurizing the matte. However, to our knowledge, there have been no reports to date concerning the sulfurization of P and Mn contained in molten slag. Therefore, knowledge of the distribution of Fe, Mn and P between the matte and the molten slag is required to determine the feasibility of this process. In this study, the equilibrium distributions of Mn, Fe, Ca and P between a FeS-MnS matte and FeO-MnO-SiO_2-MgO-P_2O_5 slag with/without CaO are investigated under controlled partial pressures of oxygen and sulfur. It was found, as P is not present in the matte, that a separation of P from Mn was accomplished. The increament of $(CaO + MgO)/SiO_2$ in slag can improve the concentrations of Mn and Fe in the matte. The content of Ca in the matte was less than 2 mass%, even when the concentration ratio of CaO/SiO_2 in the slag was unity.

Keywords. Recycling, steelmaking slag, manganese, phosphorus, sulfurization, separation, distribution, P_{O_2}, P_{S_2}, activity coefficient, MnS, FeS.

PACS®(2010). 05.70.-a, 64.75.-g, 88.10.jp.

1 Introduction

The physical and chemical properties of steel products are improved through the addition of appropriate alloying elements. Recently, due to the growing demand for high-grade steel products, the quality of steel products has become significantly dependent on the value of the alloying materials. Moreover, the value of alloying materials is lost in the steel recycling process because the recycled scraps are used for the manufacture of low-grade steel, regardless of alloying element content. Thus, alloying elements are important in the manufacture of high-grade steels, but are rarely recovered.

Mn is one of the most important alloying elements for steel because its addition is associated with improved mechanical properties. Indeed, Mn is considered to be an essential alloying element in various advanced steel products which require high strength and also improved formability. The increased consumption of Mn in steel has led to demands for high-purity Fe-Mn alloys with a low P content. More than 80% of Mn is produced by only five countries in the world and more than 95% of the Mn sources are in just six countries: South Africa, Ukraine, Australia, China, India and Gabon [1]. It is important that major steel producers establish stable future supplies in light of the scarcity of Mn resources in their countries. In fact, in Japan, Mn is designated as one of its national stockpile elements to stave off a potential delay in its supply to domestic steel producers. Despite the importance of this element, no attempts have been made to establish a reliable supply of Mn through the generation of an effective Mn recycling process.

In Japan, there is a domestic source of Mn contained in slag which is a by-product of the steelmaking process. During steelmaking, approximately 0.3% of the Mn content in hot metal is oxidized in a basic oxygen furnace and removed as slag. Following this, the steel undergoes a secondary steelmaking process, during which imported Fe-Mn alloys are added. And also, Mn loss occurs when the scrap is melted in an electric arc furnace and the Mn is oxidized and partially removed in the slag. As shown in Figure 1, the total amount of Mn wasted in steelmaking slag is almost equal to that consumed, in the form of Fe-Mn alloy, during the steelmaking process [2]. This means that a significant amount of Mn is wasted as a by-product of the steelmaking process. In this regard, it is important to develop a method for the effective recycling of steelmaking slag to recover these valuable Mn resources

While Mn can be recovered as a Fe-Mn alloy by reducing steelmaking slag with carbon, this simple reduction is not suitable for the production of Fe-Mn alloy from steelmaking slag because it commonly contains about 1.7 mass% P in the form of P_2O_5 [3]. Although it is possible to increase

Corresponding author: Hiroyuki Shibata, Institute of Multidisciplinary Research for Advanced Materials, Tohoku University, 2-1-1 Katahira, Aoba-ku, Sendai 980-8577, Japan; E-mail: shibata@tagen.tohoku.ac.jp.

Received: February 3, 2011. Accepted: April 15, 2011.

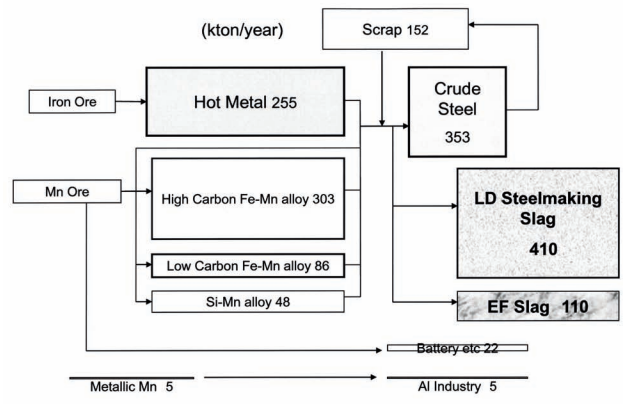

Figure 1. Material flow of manganese in Japan

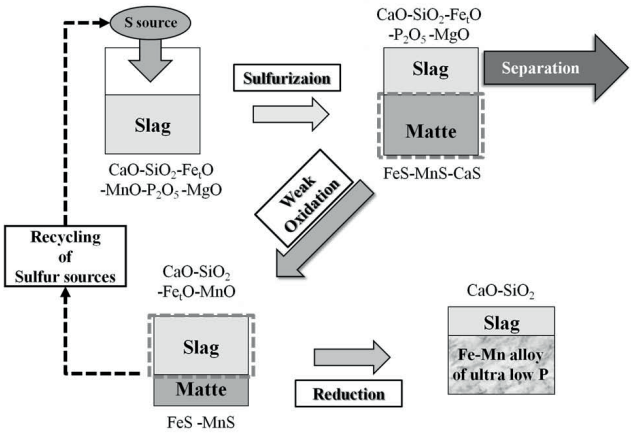

Figure 2. Schematic diagram for the proposed recycling process of Mn from slag.

up to 25% of the Mn content by carbon-based reduction, this could lead to an increase in the P concentration in the resultant Fe-Mn alloy products by 7%, as determined by a mass balance calculation. Furthermore, Matsui et al. [4] reported that more than 50% of P in the slag phase was also reduced and included in the obtained metal phase after the carbon-based reduction of steelmaking slag.

Therefore, we propose a novel recycling process for recovering Mn from steelmaking slag. Figure 2 shows a schematic diagram of the proposed process. Firstly, the Mn- and P-containing steelmaking slag is sulfurized to separate the P from the Mn, as MnS is preferentially formed in the liquid sulfide phase (matte). In this step, P remains as an oxide due to the low thermal stability of the phosphorus sulfides over 796 K [5]. The next step is to oxidize the separated matte. In this case, the ratio of Mn/Fe increases in the slag phase and the sulfur in the matte is recovered and reused in the sulfurization step. Therefore, a Fe-Mn alloy with an ultra low P content can be produced.

In order to clarify the feasibility of this process, it is necessary to investigate the distribution of Fe, Mn and P in both the matte and steelmaking slag under an atmosphere in which the partial pressures of sulfur and oxygen are controlled.

The current study presents, under the controlled atmosphere of CO-CO_2-SO_2mixing gas, the equilibrium distributions of Fe, Mn, Ca, and P between the matte and the molten slag.

2 Experimental Methods

This experiment determines the equilibrium distributions of Fe, Mn, Ca, and P in the FeS–MnS matte and the FeO-MnO-SiO_2-MgO-P_2O_5 slag system with/without CaO under a controlled $CO/CO_2/SO_2$ atmosphere at 1673 K. Figure 3 shows the experimental setup. A furnace, equipped with a Kanthal Super heating element and an alumina reaction tube (42 mm inner diameter and 1000 mm height) was used. The temperature of the sample was measured using a Pt-6%Rh/Pt-30%Rh thermocouple and maintained within ± 5 K. Approximately 5 g of slag was charged on approximately 5 g of matte in the magnesia crucible (19 mm inner diameter and 45 mm height). The slag and the matte were made by mixing the appropriate ratio of reagents. Table 1 shows the initial compositions of matte and slag. In order to make the liquid sulfide phase at 1673 K, the ratio of MnS to FeS in the matte was set at 2 : 8. Three types of slag composition were prepared, as listed in Table 1. Series 1 (S1) and 2 (S2) were investigated with respect to the effect of CaO/SiO_2on the Fe, Mn and P distribution, while series 3 (S3) was investigated with respect to the effect of the partial pressures of sulfur gas, P_{S_2}, and oxygen gas, P_{O_2}, on the distribution ratios. The preliminary experiments confirmed

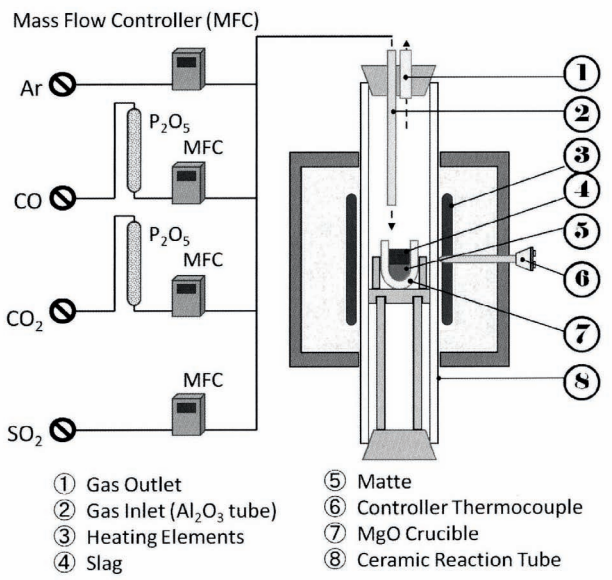

Figure 3. Experimental setup.

	Slag/ mass%						Matte / mass%	
	CaO	SiO_2	FeO	MnO	MgO	P_2O_5	FeS	MnS
S1	21	41	12	12	9	5		
S2	31	31	12	12	9	5	80	20
S3		40	20	20	15	5		

Table 1. Initial compositions of slag and matte.

that the reaction achieved equilibrium after 24 h when the Mn and Fe distributions between the matte and the slag became constant.

The sample was heated at 1673K under a suitable $CO/CO_2/SO_2$ atmosphere in a furnace. The flow rate of the CO and CO_2 gasses were about $70–139 \times 10^{-6}$ m^3/min and $0.9–80 \times 10^{-6}$ m^3/min, respectively. P_{S_2} was controlled to be $P_{S2} \geq 10^{-3}$ [atm] and $P_{S_2} \leq 10^{-4}$ [atm] in the ranges of $2–20 \times 10^{-6}$ m^3/min for SO_2 gas and $0.4–9.1 \times 10^{-6}$ m^3/min for Ar-1%SO_2 gas, respectively. The equilibrium relation between P_{S_2} and P_{O_2} was calculated using the following equations:

$$2CO(g) + O_2(g) = 2CO_2(g), \quad (1)$$
$$\Delta G^\circ \text{ (J/mol)} = -565\,160 + 172.03T,$$
$$1/2S_2(g) + O_2(g) = SO_2(g), \quad (2)$$
$$\Delta G^\circ \text{ (J/mol)} = -361\,660 + 72.48T.$$

Figure 4 shows the potential diagram calculated using thermodynamic data [6]. In this figure, the equilibrium P_{O_2} and P_{S_2} of reactions (3) to (6) at 1673 K are indicated, with the various reactions of the oxides and sulfides taken into consideration.

$$2Fe(s) + O_2(g) = 2FeO(l), \quad (3)$$
$$\Delta G^\circ \text{ (J/mol)} = -477\,560 + 97.06T,$$
$$2Fe(s) + S_2(g) = 2FeS(l), \quad (4)$$
$$\Delta G^\circ \text{ (J/mol)} = -240\,670 + 69.16T,$$
$$2Mn(l) + O_2(g) = 2MnO(l), \quad (5)$$
$$\Delta G^\circ \text{ (J/mol)} = -713\,300 + 129.6T,$$
$$2Mn(l) + S_2(g) = 2MnS(s), \quad (6)$$
$$\Delta G^\circ \text{ (J/mol)} = -593\,390 + 153.17T.$$

As shown in Figure 4, the experimental conditions of low P_{S_2} and P_{O_2} are indicated by series 1 in which the metal phase (iron) can form, while series 2 indicates relatively high P_{S_2} and P_{O_2} The MgO crucible with the sample was removed from the furnace after 24 h and then quenched in water.

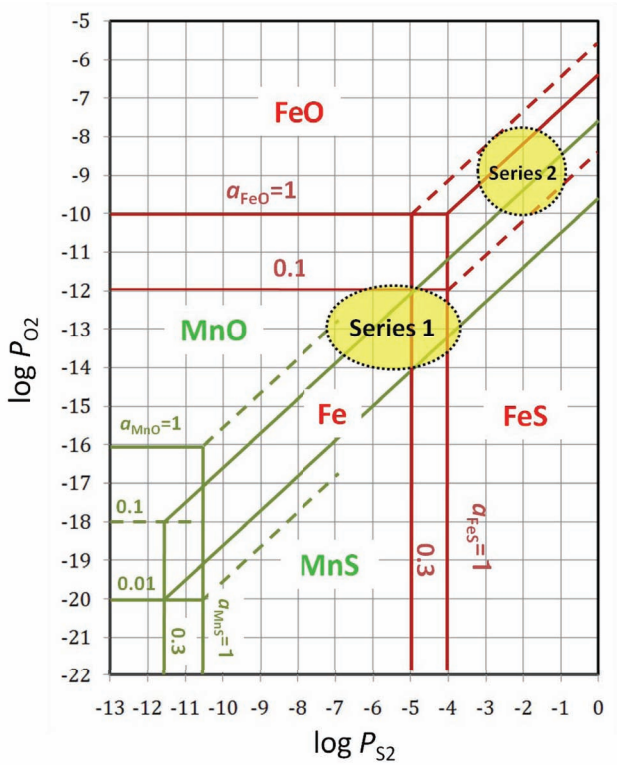

Figure 4. Fe and Mn speciation diagram with respect to log P_{O_2} and log P_{S_2} for series 1 and 2 at 1673 K.

The amounts of Fe, Mn, Mg, Ca and P were analyzed using inductive coupled plasma-atomic emission spectroscopy (ICP-AES, Optima 3300). Assuming that FeO, MnO, MgO and P_2O_5 are the oxide components of the S3 slag, the SiO_2 content was calculated by subtracting the sum of these components from 100 mass%. In the case of the S1 and S2 slag, the Si content in slag was measured using ICP-AES and a gravimetric method with alkali-fusion. The microstructures and compositions of the matte and slag were observed using an electron probe micro analyzer (EPMA, JXA-8200). The sulfur content of the slag was measured using infrared absorption spectroscopy (IR, EMIA-520) to determine the amount of suspended sulfide in the slag.

Run	$logP_{O2}$	$logP_{S2}$	Matte / {mass%}					Slag / (mass%)						
			{Fe}	{Mn}	{Ca}	{Mg}	{P}	(Fe)	(Mn)	(Mg)	(P)	(Ca)	(Si)	(S)
S1	-13	-6	54.5	13.5	1	0.5	0.1	7.3	9.8	10.8	2.1	15.6	18.4	1.4
S2	-13	-6	53.9	16.1	1.9	0.2	< 0.1	6	6.8	10.2	2.2	21.1	14.4	2.2
J	-12	-5	57.2	12.2		0.1	< 0.1	12.9	19.9	12.4	2.2		15.0	2.8
K	-13	-4	57.2	11.9		0.2	< 0.1	14.6	15.8	11.9	2.1		16.9	3.5
L	-13	-5	57.3	12.5		0.2	< 0.1	13.5	17	11.9	2		17.0	2.7
M	-13	-6	60	12.4		0.3	< 0.1	12.5	17.5	12.8	2.3		16.3	2.0
N	-13	-7	58.9	11.6		< 0.1	< 0.1	13.6	19.3	12.2	2		15.4	2.4

Table 2. Experimental results for series 1.

3 Results

3.1 Series 1 Equilibrium Ratio Between FeS-MnS Matte and FeO-MnO-SiO_2-CaO-MgO-P_2O_5 Slag

Table 2 shows the experimental results of Series 1 in Figure 4. The content of P in the matte was almost always less than 0.1 mass% (i.e. less than the lower limit of the analysis method). It was confirmed that the P can be separated from Fe and Mn by the formation of a liquid sulfide phase (matte). The content of Ca in the matte was less than 2 mass%, even though the content of CaO was approximately 30% in the S2 slag.

However, sulfide and oxide particles are evident within the slag and matte, respectively, as shown in Figures 5 and 6. The compositions of the sulfide and oxide particles, which were analyzed by EPMA, are similar to the matte and slag phases respectively. Therefore it can be found that they are not precipitated particles but the suspended particles.

The total amount and composition of suspended sulfide within slag can be determined by the detected composition of sulfide particles with EPMA and the total contents of S in slag with IR. The revised slag compositions were therefore calculated by subtracting the amount of each element in the suspended sulfide particles from the chemical analysis results of slag phase in Table 2. On the other hand, the content of Mg in matte resulted from the suspended oxide particles within matte. In the same way, the total amount and composition of suspended oxides within the matte can be defined by the detected composition of suspended oxide particles and the total Mg content in the matte. Hence, the matte composition can be also obtained by substrcating the amount of each element in the suspended oxide particles from the chemical analysis results of matte phase in Table 2.

Table 3 shows the compositions of the slag and matte after revising the suspended phases. In this table, the content of each element in slag was converted to the oxide and that in matte was converted to the sulfide. As shown in Figure 7, the total amount of slag suspended in the matte was 0.1–5 mass% and was independent of the composition of matte shown in Table 3. The total amount of suspended matte within the slag was also independent of the slag composition, as shown in Figure 8.

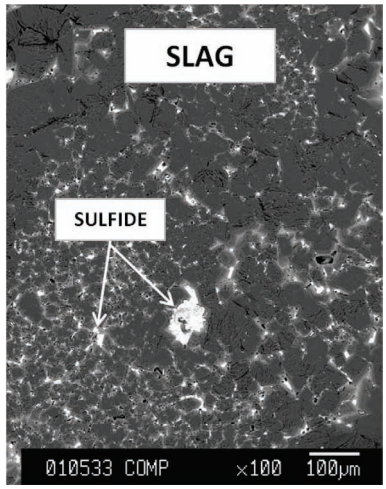

Figure 5. Suspended sulfides within slag.

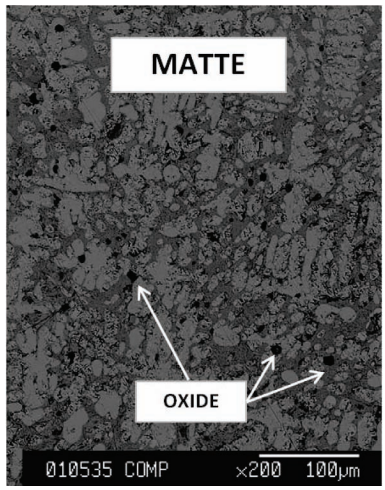

Figure 6. Suspended oxides within matte.

In this experiment, the degree of freedom is calculated to be 7 because the system consists of 9 elements (Fe, Mg, Si, Mg, P, C, S, O and Ca) and 4 phases (gas, molten slag, molten matte, and crucible), using the phase rule. Hence, the temperature, total pressure, CO/CO_2, SO_2/S_2,

Run	$\log P_{O2}$	$\log P_{S2}$	Matte / {mass%}			Slag / (mass%)					
			FeS	MnS	CaS	FeO	MnO	MgO	P_2O_5	CaO	SiO_2
S1	-13	-6	79.9	19.6	0.5	6.7	12.0	17.5	4.6	21.1	38.1
S2	-13	-6	75.3	22.7	2.0	3.7	7.7	18.2	5.4	31.7	33.2
J	-12	-5	82.5	17.5		10.6	27.4	22.8	5.6		33.6
K	-13	-4	82.9	17.1		14.5	19.6	22.1	5.4		38.5
L	-13	-5	82.3	17.7		13.4	22.2	21.5	5.0		37.9
M	-13	-6	83.1	16.9		13.5	22.3	22.7	5.6		35.9
N	-13	-7	83.5	16.5		14.1	25.3	21.8	4.9		33.9

Table 3. Matte and slag compositions of series 1 after revising the suspended phases.

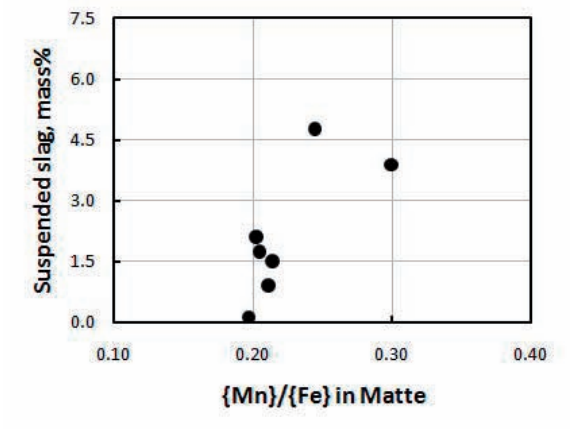

Figure 7. Total amount of suspended slag within matte as a function of {Mn}/{Fe} of matte in Table 3.

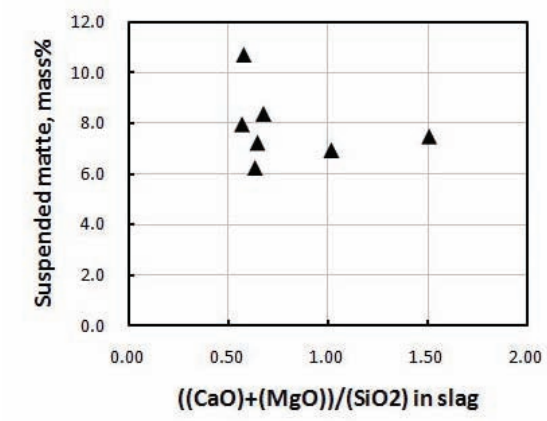

Figure 8. Total amount of suspended matte within slag as a function of $(CaO + MgO)/SiO_2$ of slag in Table 3.

MgO (saturated in slag), mass% of P_2O_5 in the slag and CaO/SiO_2 in the slag were set so that an equilibrium was able to be achieved.

For this reason, Figure 9(A) and (B) shows the relationship between $(CaO + MgO)/SiO_2$ and the obtained compositions in Table 3 where P_{O_2} (CO/CO_2) and P_{S_2} (SO_2/S_2) are between 10^{-12} [atm] and 10^{-13} [atm] and between 10^{-5} [atm] and 10^{-7} [atm], respectively. As shown in Figure 9(A), the ratio of Mn/Fe in the matte and that in the slag increased as the $(CaO + MgO)/SiO_2$ ratio increased. However, in every case, the ratio of Mn/Fe in the matte was below 0.4 and lower than that in the slag. In addition, based on the phase diagram [7], the ratio of Mn/Fe in liquid phase at 1673 K is less than 0.4 in the binary FeS-MnS system. This implies that, at 1673 K, the content of Mn in matte cannot be condensed.

Figure 9(B) shows the partition ratios of Fe and Mn between the matte and the slag, which are expressed by the following equation:

$$\text{Partition ratio} = \frac{\{\text{mass\% M in matte}\}}{(\text{mass\% M in slag})}, \qquad (7)$$

where M means Fe or Mn.

Both partition ratios increased with an increasing $(CaO + MgO)/SiO_2$ ratio and the partition ratio of Fe was always higher than that of Mn. These results indicate that Fe sulfides are more readily formed than Mn sulfides. It is also expected that the activity of MnS is much higher than that of FeS under the partial pressure conditions of series 1.

3.2 Series 2 Equilibrium Ratio Between the FeS-MnS Matte and FeO-MnO-SiO_2-MgO-P_2O_5 Slag

In this experiment, the degree of freedom is 6 because the system consists of 8 elements (Fe, Mg, Si, Mg, P, C, S and O) and 4 phases (gas, molten slag, molten matte, and crucible). In order to maintain the equilibrium, the temperature, total pressure, CO/CO_2, SO_2/S_2, MgO (saturated) and mass% P_2O_5 in slag were set.

Table 4 shows the experimental results of series 2. The contents of P in the matte were nearly always less than 0.1 mass%, which is similar to the results determined for series 1, as shown in Table 2. It is clear that the sulfurization of molten slag forms the sulfides of Fe and Mn, but not of P, and the separation of P is not related to the P_{S_2} and P_{O_2}.

Run	$\log P_{O2}$	$\log P_{S2}$	Matte / {mass%}				Slag / (mass%)					
			{Fe}	{Mn}	{Mg}	{P}	(Fe)	(Mn)	(Mg)	(P)	(Si)	(S)
A	-8.3	-1.6	49.4	11.6	0.1	< 0.1	22.0	16.8	6.8	1.5	15.6	3.7
B	-9.0	-1.1	49.5	13.7	< 0.1	< 0.1	9.3	8.6	9.8	2.3	25.0	3.5
C	-8.8	-1.6	50.0	11.7	< 0.1	< 0.1	14.0	15.2	8.9	2.5	19.0	2.3
D	-8.5	-2.1	47.4	10.9	0.2	< 0.1	16.5	14.6	10.3	1.6	17.8	2.1
E	-9.4	-1.2	46.2	13.5	< 0.1	< 0.1	8.1	11.2	12.0	1.7	23.7	1.3
F	-9.3	-1.4	46.8	14.1	< 0.1	< 0.1	11.6	8.2	12.1	1.9	22.9	2.0
G	-8.8	-2.4	50.0	11.4	< 0.1	0.1	25.1	15.3	6.8	1.2	14.9	4.1
H	-9.8	-1.4	46.4	14.1	< 0.1	< 0.1	6.4	8.7	11.7	1.6	26.4	1.9
I	-9.6	-1.7	50.8	10.8	0.2	< 0.1	15.6	14.5	10.0	2.0	18.3	1.8

Table 4. Experimental results for series 2.

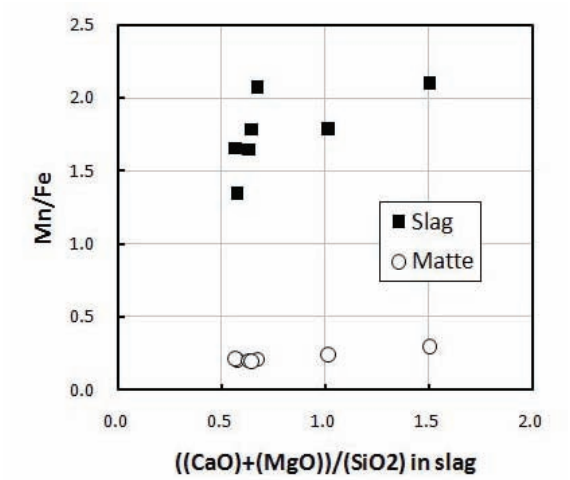

(A) Ratio of Mn/Fe in matte and slag

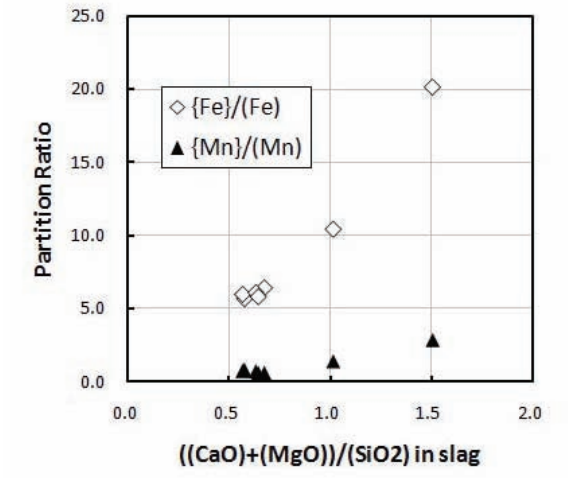

(B) Partition ratios of Fe and Mn between matte/slag

Figure 9. Relationship between $(CaO + MgO)/SiO_2$ and the composition of matte and slag, as shown in Table 3, where P_{O_2} (CO/CO_2) and P_{S_2} (SO/SO_2) are 10^{-12}–10^{-13} and 10^{-5}–10^{-7}.

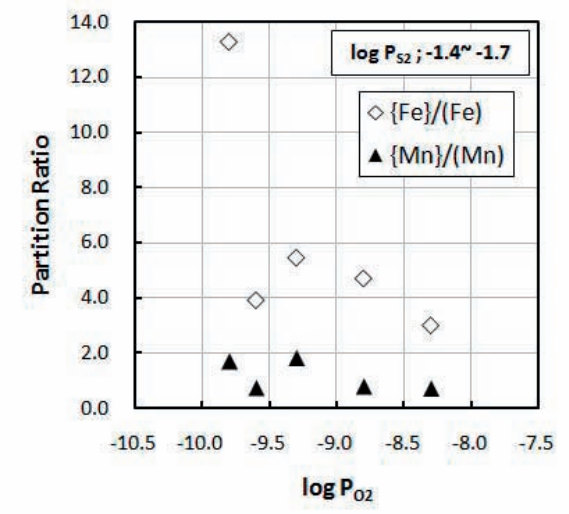

(A) Effect of P_{O_2}

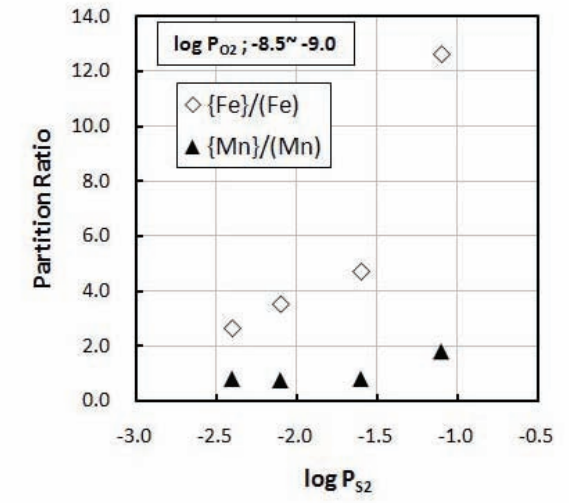

(B) Effect of P_{S_2}

Figure 10. Effects of P_{O_2} or P_{S_2} on the partition ratios of Fe and Mn between matte/molten slag.

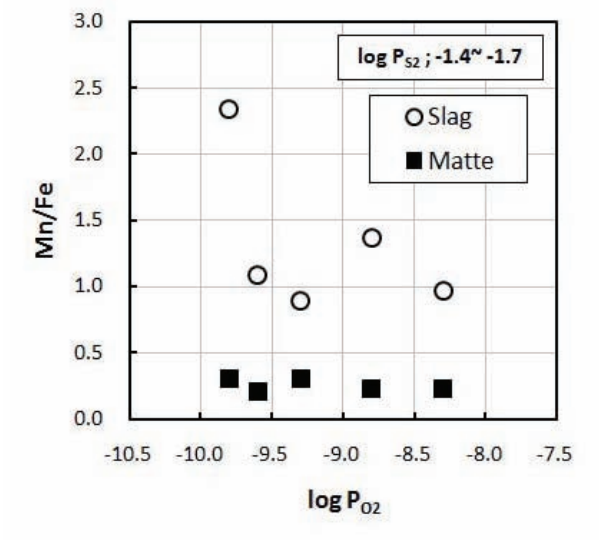

(A) Effect of P_{O_2}

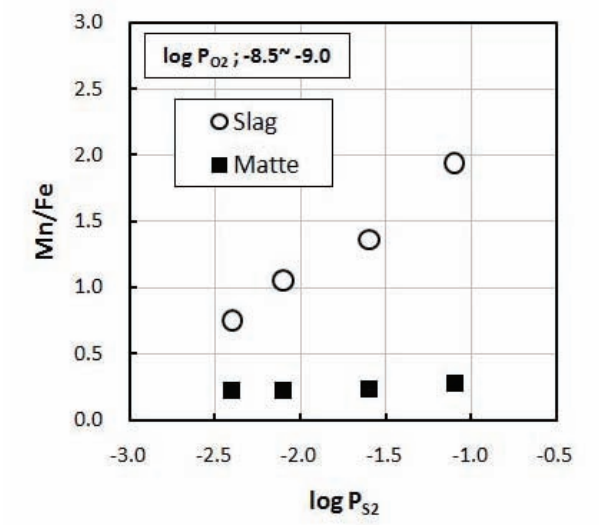

(B) Effect of P_{S_2}

Figure 11. Effect of P_{O_2} or P_{S_2} on the content ratio of Mn/Fe in matte and slag.

By using the same calculation as series 1, the equilibrium compositions of series 2 can be also obtained, as shown in Table 5. Figure 10(A) shows the effect of P_{O_2}, at a constant P_{S_2}, on the partition ratio of Fe and Mn between the matte/slag, while Figure 10(B) presents the corresponding effect of P_{S_2}, at a constant P_{O_2}. It is evident that the partition ratios of Fe and Mn between the matte and the molten slag increased as the P_{S_2} increased and the P_{O_2} decreased. Furthermore, Figure 11(A) and (B) shows the effect of P_{O_2} or P_{S_2} on the ratio of Mn/Fe in the matte and slag. The ratio of Mn/Fe in the matte and slag shows a similar trend with increasing P_{S_2} and decreasing P_{O_2}.

4 Discussion

Table 6 shows the mole fractions of matte and slag for series 1 and 2. The relationship of partition ratio of Fe and Mn between the matte and the slag can be represented by the following equations:

$$\begin{aligned} &\mathrm{FeO(l)} + 1/2\mathrm{S_2} = \mathrm{FeS(l)} + 1/2\mathrm{O_2}, \\ &\Delta G^\circ\ (\mathrm{J/mol}) = 118\,445 - 13.95T, \end{aligned} \tag{8}$$

$$\frac{\gamma_{\mathrm{FeS}}}{\gamma_{\mathrm{FeO}}} \times \frac{N_{\mathrm{FeS}}}{N_{\mathrm{FeO}}} \times \left(\frac{P_{\mathrm{O_2}}}{P_{\mathrm{S_2}}}\right)^{1/2} = K_8, \tag{9}$$

$$\begin{aligned} \log \frac{N_{\mathrm{FeS}}}{N_{\mathrm{FeO}}} = &-\frac{1}{2}\log P_{\mathrm{O_2}} + \frac{1}{2}\log P_{\mathrm{S_2}} \\ &- \log \frac{\gamma_{\mathrm{FeS}}}{\gamma_{\mathrm{FeO}}} + \log K_8, \end{aligned} \tag{10}$$

$$\begin{aligned} &\mathrm{MnO(l)} + 1/2\mathrm{S_2} = \mathrm{MnS(s)} + 1/2\mathrm{O_2}, \\ &\Delta G^\circ\ (\mathrm{J/mol}) = 59\,955 + 11.783T, \end{aligned} \tag{11}$$

$$\frac{\gamma_{\mathrm{MnS}}}{\gamma_{\mathrm{MnO}}} \times \frac{N_{\mathrm{MnS}}}{N_{\mathrm{MnO}}} \times \left(\frac{P_{\mathrm{O_2}}}{P_{\mathrm{S_2}}}\right)^{1/2} = K_{11}, \tag{12}$$

$$\begin{aligned} \log \frac{N_{\mathrm{MnS}}}{N_{\mathrm{MnO}}} = &-\frac{1}{2}\log P_{\mathrm{O_2}} + \frac{1}{2}\log P_{\mathrm{S_2}} \\ &- \log \frac{\gamma_{\mathrm{MnS}}}{\gamma_{\mathrm{MnO}}} + \log K_{11}. \end{aligned} \tag{13}$$

When either P_{O_2} or P_{S_2} is constant and the ratio of the activity coefficient ($\gamma_{\mathrm{FeS}}/\gamma_{\mathrm{FeO}}$ or $\gamma_{\mathrm{MnS}}/\gamma_{\mathrm{MnO}}$) in equations (10) and (13) is constant, the mole fraction ratio of Fe and Mn between matte/slag is practically proportional to $-1/2$ of $\log P_{O_2}$ and $1/2$ of $\log P_{S_2}$, as shown in Figure 12(A) and (B), respectively. Moreover, by combining equations (9) and (11), equation (15) is derived, which can be used to express the ratio of Mn/Fe in the matte and the slag:

$$\begin{aligned} &\mathrm{FeO(l)} + \mathrm{MnS(s)} = \mathrm{FeS(l)} + \mathrm{MnO(l)}, \\ &\Delta G^\circ\ (\mathrm{J/mol}) = 58\,490 - 25.735T, \end{aligned} \tag{14}$$

$$\frac{N_{\mathrm{FeS}}}{N_{\mathrm{MnS}}} \times \frac{N_{\mathrm{MnO}}}{N_{\mathrm{FeO}}} \times \frac{\gamma_{\mathrm{FeS}}}{\gamma_{\mathrm{MnS}}} \times \frac{\gamma_{\mathrm{MnO}}}{\gamma_{\mathrm{FeO}}} = K_{14}. \tag{15}$$

In equation (15) K_{14} is the equilibrium constant at 1673 K and ($N_{\mathrm{FeS}}/N_{\mathrm{MnS}}$) and ($N_{\mathrm{MnO}}/N_{\mathrm{FeO}}$) terms indicate the mole fraction ratios of FeS and MnS in the matte and of FeO and MnO in the slag, respectively. The terms ($\gamma_{\mathrm{FeS}}/\gamma_{\mathrm{MnS}}$) and ($\gamma_{\mathrm{MnO}}/\gamma_{\mathrm{FeO}}$) refer to the activity coefficient ratios of MnS and FeS in the matte and of MnO and FeO in the molten slag, respectively.

Figure 13 shows the change in ($N_{\mathrm{FeS}}/N_{\mathrm{MnS}}$) × ($N_{\mathrm{MnO}}/N_{\mathrm{FeO}}$) as a function of P_{O_2} or P_{S_2}, even though the partial pressures of oxygen and sulfur are not independent variables. As shown in Figure 13, the values of ($N_{\mathrm{FeS}}/N_{\mathrm{MnS}}$) × ($N_{\mathrm{MnO}}/N_{\mathrm{FeO}}$) in series 1 were relatively higher than those of series 2. As mentioned above, both the P_{S_2} and P_{O_2} in series 1 are higher than those in series 2.

Run	$logP_{O2}$	$logP_{S2}$	Matte / mass%		Slag / mass%				
			FeS	MnS	FeO	MnO	MgO	P_2O_5	SiO_2
A	-8.3	-1.6	81.1	18.9	23.5	22.8	12.6	3.8	37.3
B	-9.0	-1.1	78.3	21.7	5.6	10.9	18.1	5.8	59.6
C	-8.8	-1.6	81.0	19.0	14.6	20.0	15.8	6.1	43.5
D	-8.5	-2.1	81.6	18.4	18.2	19.2	18.2	3.9	40.5
E	-9.4	-1.2	77.3	22.7	8.2	14.5	20.7	4.0	52.6
F	-9.3	-1.4	76.8	23.2	11.6	10.5	21.3	4.6	52.0
G	-8.8	-2.4	81.4	18.6	27.4	20.7	12.8	3.1	36.0
H	-9.8	-1.4	76.6	23.4	4.7	11.1	20.5	3.9	59.7
I	-9.6	-1.7	82.7	17.3	17.4	19.0	17.5	4.8	41.2

Table 5. Matte and slag compositions of series 2 after revising the suspended phases.

	Run	$logP_{O2}$	$logP_{S2}$	Matte /mole fraction			Slag / mole fraction					
				N_{FeS}	N_{MnS}	N_{CaS}	N_{FeO}	N_{MnO}	N_{MgO}	N_{P2O5}	N_{CaO}	N_{SiO2}
Series 1	S1	-13	-6	0.80	0.20	0.01	0.05	0.09	0.25	0.02	0.22	0.37
	S2	-13	-6	0.75	0.23	0.02	0.03	0.06	0.26	0.02	0.32	0.31
	J	-12	-5	0.82	0.18		0.09	0.23	0.33	0.02		0.33
	K	-13	-4	0.83	0.17		0.12	0.16	0.32	0.02		0.38
	L	-13	-5	0.82	0.18		0.11	0.18	0.31	0.02		0.37
	M	-13	-6	0.83	0.17		0.11	0.18	0.33	0.02		0.35
	N	-13	-7	0.83	0.17		0.12	0.21	0.32	0.02		0.33
Series 2	A	-8.3	-1.6	0.81	0.19		0.20	0.20	0.19	0.02		0.39
	B	-9.0	-1.1	0.78	0.22		0.05	0.09	0.26	0.02		0.58
	C	-8.8	-1.6	0.81	0.19		0.12	0.17	0.24	0.03		0.44
	D	-8.5	-2.1	0.81	0.19		0.15	0.16	0.27	0.02		0.40
	E	-9.4	-1.2	0.77	0.23		0.07	0.12	0.30	0.02		0.50
	F	-9.3	-1.4	0.77	0.23		0.09	0.08	0.30	0.02		0.50
	G	-8.8	-2.4	0.81	0.19		0.24	0.18	0.20	0.01		0.37
	H	-9.8	-1.4	0.76	0.24		0.04	0.09	0.29	0.02		0.57
	I	-9.6	-1.7	0.83	0.17		0.15	0.16	0.26	0.02		0.41

Table 6. Mole fractions of matte and slag for series 1 and 2.

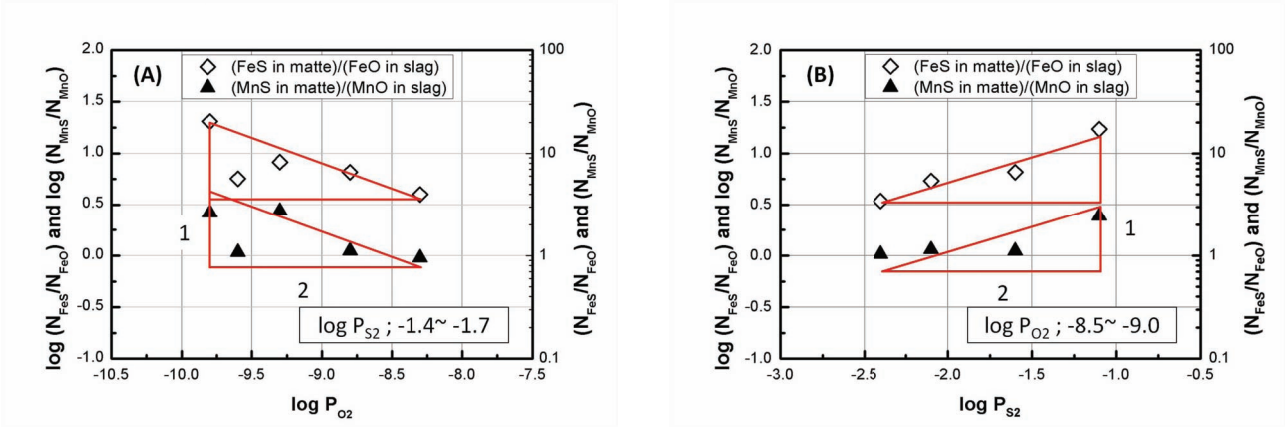

Figure 12. Relations of P_{O_2} (A) and P_{S_2} (B) with logarithmic mole fraction ratios of Fe and Mn between matte/slag.

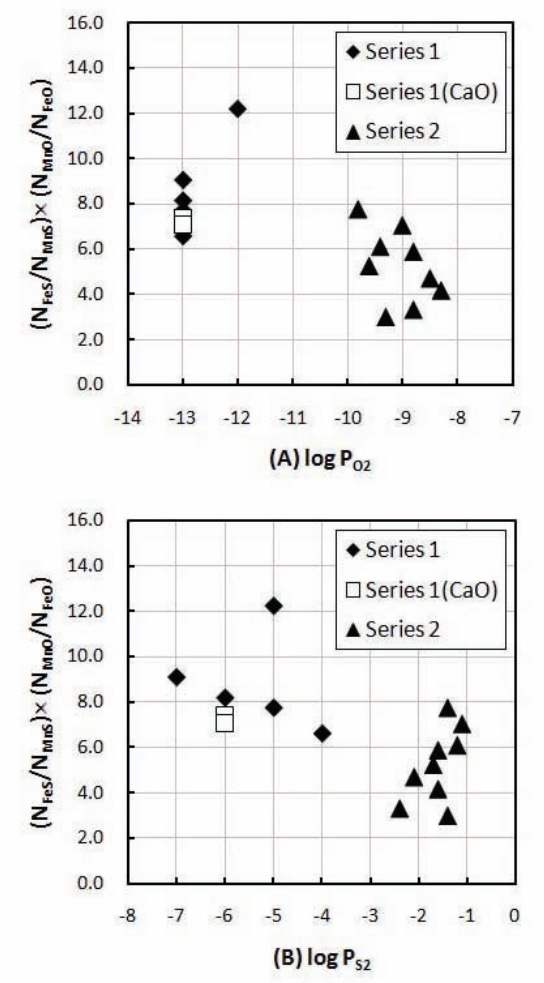

Figure 13. Relation of P_{O_2} (A) and P_{S_2} (B) with the change of $(N_{FeS}/N_{MnS}) \times (N_{MnO}/N_{FeO})$.

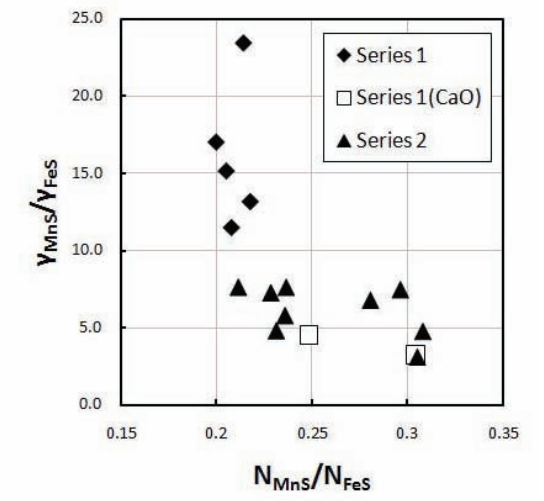

Figure 14. Relationship netween the ratio of $(\gamma_{MnS}/\gamma_{FeS})$ and that of (N_{MnS}/N_{FeS}) in matte.

This implies that $(\gamma_{FeS}/\gamma_{MnS}) \times (\gamma_{MnO}/\gamma_{FeO})$ is not constant value and changed by the experimental conditions. The values of $(\gamma_{FeS}/\gamma_{MnS})$ were evaluated by using regular solution model [8] which calculated the values of $(\gamma_{MnO}/\gamma_{FeO})$ in equation (15).

Figure 14 shows the relationship between the ratio of $(\gamma_{MnS}/\gamma_{FeS})$ and that of (N_{MnS}/N_{FeS}) in the matte. The ratio of $(\gamma_{MnS}/\gamma_{FeS})$ increased exponentially while that of (N_{MnS}/N_{FeS}) in the matte decreased below approximately 0.22. Furthermore, in every case, the values of γ_{MnS} were more than 3 times larger than that of γ_{FeS}. For this reason, the partition ratios of Fe between the matte/slag were consequently higher than that of Mn.

5 Conclusion

We have proposed a novel recycling process to recover Mn from steelmaking slag via sulfurization to separate P from Fe and Mn. In order to evaluate the feasibility of this process, the equilibrium distributions of Fe, Mn and P between the liquid sulfide (matte) and molten slag at 1673 K were investigated.

The conclusions of the present study are as follows:

I. The content of P in the matte was almost always less than 0.1 mass%. It was revealed that P was not present in the matte and thus separation of P from Mn was achieved.

II. The ratio of $(CaO + MgO)/SiO_2$ in the slag affects the Mn and Fe content in the matte. The content of Ca in the matte was less than 2 mass%, even when the ration of CaO/SiO_2 was unity in the slag.

III. The partition ratios of Mn and Fe between the matte/slag were proportional to $1/2$ of $\log P_{S_2}$ and $-1/2$ of $\log P_{O_2}$, respectively.

IV. By calculating the activities of FeO and MnO in the molten slag using the regular solution model, the relationship between the ratio of $(\gamma_{MnS}/\gamma_{FeS})$ and that of Mn/Fe in matte was found.

V. In every case, the ratio of Mn/Fe in the matte did not exceed 0.3 at 1673 K. This implies that sulfurization of the molten slag is not sufficient to improve the ratio of Mn/Fe in the matte at 1673 K.

The above conclusions suggest that the separation of P from Fe and Mn by the sulfurization of steelmaking slag is a feasible first step in our proposed recycling process. We are currently investigating the effects of the slag composition, P_{S_2}, and P_{O_2} on the the distribution of Mn and Fe in the matte in detail. The next step of our proposed process is to oxdize and desufurize the matte and thus improve the ratio of Mn/Fe for the production of highpurity Fe-Mn alloys.

Acknowledgments

The authors appreciate the financial support of the Japan Society for the Promotion of Science (Grant-in-Aid for Scientific Research (B)), the Sumitomo Foundation and Steel Industry Foundation for the Advancement of Environmental Protection Technology. This work was also partially supported by the Global COE Program "Materials Integration, Tohoku University," MEXT, Japan. This work was also partially supported by University Facility Network Program of Institute for Molecular Science.

References

[1] Mineral Commodity Summaries of U.S. Geological Survey, 2008–2009.

[2] K. Nakajima, K. Yokoyama and T. Nagasaka, Substance flow analysis of manganese associated with iron and steel flow in Japan, *ISIJ International*, **48**, No. 4 (2008), 549–553.

[3] `http://slg.jp/slag/slag-_seisitsu.htm`, Nippon Slag Association: Chemical Composition of Iron and Steel Slag.

[4] A. Matsui, N. Kikuchi, Y. Kishimoto and K. Takahashi, Fundamental study on phosphorus separation and collection from steel making slag, *CAMP-ISIJ*, **23** (2010), 901.

[5] A. H. Cowley, The structures and reactions of the phosphorurs sulfides, *J. Chem. Educ.*, **41**, No. 10 (1964), 530–534.

[6] O. Knacke, O. Kubaschewski and K. Hesselmann, *Thermochemical Properties for Inorganic Substances*, 2nd edn., Springer-Verlag, Verlag Stahleisen (1991).

[7] V. Raghavan, *Phase Diagrams of Ternary Iron Alloys, Part 2*, The Indian Institute of Metals, Calcutta (1988).

[8] S. Ban-ya, Mathematical expression of slag-metal reactions in steelmaking process by quadratic formalism based on the regular solution model, *ISIJ International*, **33**, No. 1 (1993), 2–11.